

Synthesis, Characterization of InP Nanospheres and Fabrication of InP Nanofibers by Electrospinning Method

Shomaila Saeed*, Muhammad Umer

Quaid-i-Azam University, Department of Chemistry, Islamabad 45320, Pakistan.

* **Corresponding Author:** Email: Shomaila.nafees@gmail.com

Abstract

We report a unique route for synthesis of Indium Phosphide (InP) nanostructures of different morphologies (nanospheres and nanofibers) by reaction of the Indium precursor with yellow phosphorus. Produced nanofibers are collected on fluorine doped tin oxide (FTO) coated glass substrate and preserved in a desiccator since Polyacrylonitrile (PAN) is moisture sensitive. Ozone etching is carried out to obtain InP nanofibers. The synthesized nanostructures were characterized by powder Scanning electron microscope (SEM), Atomic force microscope (AFM), X-ray diffraction (XRD), steady state photoluminescence spectroscopy (SSPL), time resolved photoluminescence spectroscopy (TRPL) and UV-Vis absorption spectroscopy. From these measurements InP Nanospheres are observed to exhibit the blue shift of about 292 nm as compared to the bulk InP 918 nm absorption value estimated band gap of synthesized InP nanospheres is ~ 1.98 eV which is larger than the band gap of bulk InP 1.34 eV. Nanostructured InP is found to exhibit zinc-blende structure with average crystallite 153 nm size, FTO supported InP nanofibers calcined at 400 °C and the fibers stiffness is analyzed by AFM that describes important properties of nanofibers, such as hardness, elastic modulus and the adhesion between nanofibers and substrate.

Keywords: Nanospheres, nanofibers, solvothermal method, capping agent, electrospinning, sonication, homogeneous dispersion, polymer matrix, Ozone etching

Introduction

InP belongs to the III-V semiconducting materials. Now a days it is attracting extensive interest of the scientific community because of its variety of applications in optical, electrical as well as the telecommunication devices [1]. Many InP based devices are being used to produce photon detectors [2], lasers [3], photon filters [4] and optical waveguides [5]. We report in this article about InP nanosphere and the InP nanofibers, which are of great scientific and technological significance. They have potential applications in fiber optics, communications, phonon detector and many other high speed electronic devices [6]. InP having a direct band gap in visible range at room temperature i.e. 1.35 eV depicting its record efficiency in solar cell devices [7]. The basic crystal structure of InP is the zinc blende structure i.e. face centered cubic as that of zinc sulphide and gallium nitride. Wurtzite i.e. the hexagonal structure of InP is also reported, but it is formed only under strong external conditions. Both structures of InP have different electronic band gaps. It also shows remarkable optical properties in addition to the electrical properties [8].

The material shows remarkable properties when its size becomes smaller due to the quantum

confinement effects [9]. This means that the motion of a freely moving electron is confined to certain specific discrete energy levels. When the size of the particle further decreases in nanometer scale the dimensions are decreased so as to enhance the confinement effects. And the energy levels become discrete and as a result of this the band becomes wider so that relationship between the band gap energy varies as a function of dimension of nanostructures [10].

Nanofibers are the fibers with at least one dimension in nanometer range. There is a wide variety of the fields in which the nanofibers are used. They are used in many of the energy transport pathways [11], photonic waveguides [12], magnetic devices [13], and sensors [14] in medical applications [15], drug delivery systems [16], scaffold formation [17], wound healing [18] and widely used in tissue engineering [19], skeletal tissue, bone tissue, cartilage tissue, ligament tissue, blood vessel tissue, neural tissue etc. It is also used in dental and orthopedic implants [20]. The nanofibers are formed by a number of techniques conventionally here we use Electrospinning process in which the electrostatic force is used to synthesize the nanofibers. Electrospinning is capable of producing ultra-fine fibers with diameters in the nanometer range (less

than 50 nm), Syringe-needle based electrospinning has been extensively explored over the last decade to make isotropic or aligned polymeric nanofiber mats for electronic [21] and biomedical applications [22]. The alignment of electro-spun fibers is effected by the orientation of the collector. The morphology and other properties are also affected by the type or design of the collector. Electrospinning technique is affected by Molecular weight, Solution Viscosity [23]. Surface tension [24], Solution conductivity [25], and Dielectric effect of solvent [26]. Processing parameters affecting electrospinning are Voltage [25], Feed rate [27], Temperature [25].

AFM is a well-known technique used to obtain topography and surface contrast images of polymers and biological samples [28].

The present work emphasizes only on the solution phase synthesis techniques for the fabrication of InP based nanostructures. InP nanospheres are synthesized by solvothermal method using indium powder and yellow phosphorous as starting reactants, toluene as solvent and Cetyltrimethylammonium bromide (CTAB) introduced as a capping agent these nanospheres are now used further with PAN to make InP/PAN composite fibers by electrospinning at 25 kV voltage and at 15 cm height with a constant precursor flow rate of 0.1 mLh⁻¹. InP/PAN nanospheres composite solutions are sonicated for 12 hours for thorough and homogeneous dispersion of InP nanomaterial in the polymer matrix. The objectives of our discussions are exploring new methods for the synthesis of InP based nanostructures, fabrication of InP nanofibers by electrospinning method, effect of ultrasonic irradiation on aggregated nanostructures, ozone etching on InP based nanofibers, stiffness and surface adhesion strength of InP nanofiber by means of AFM, and life time decay effect on nanostructures morphology.

2. Experimental

2.1 Fabrication of InP nanospheres

InP nanospheres were synthesized by solvothermal method. 3.0 mmol of yellow phosphorous was added to toluene in dry box as yellow phosphorous is highly flammable when exposed to air. The resulting solution was sonicated for 1 hour and 3.0 mmol of CTAB (Aldrich) was added as a stabilizer as well as for size sorting. 3.0 mmol of indium powder (Aldrich) was added to this solution and the solution mixture was transferred to the stainless steel teflon lined autoclave with a filling ratio of 70:30. The

solution was heated at 200 °C for 72 hours and then the autoclave was allowed to cool at room temperature. Finally, the yellow brown product was collected and washed by 1:4 ratio of acetone and chloroform solution and then by toluene, ethanol, methanol, and deionized water respectively. The final product was dried at 60 °C.

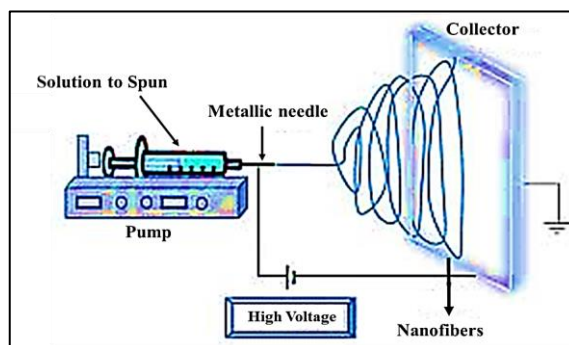


Fig. 1: Schematic of the electrospinning setup

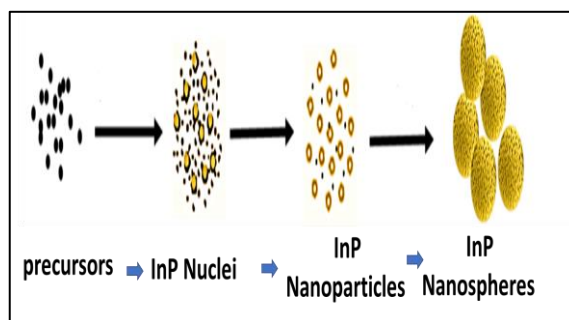


Fig. 2: Mechanism to describe the growth of InP nanospheres

2.2 Fabrication of polymer composite (InP/PAN) nanofibers

Polymer composite (InP-PAN) nanofibers were fabricated in order to yarn the InP nanofibers by electrospinning method. The solution with optimal concentration was prepared by dissolving 9 wt% of PAN ($M_w = 1.5 \times 10^5$) in N, N-Dimethyl formamide (DMF) (Aldrich) at 60 °C. The polymer solution was stirred for 24 hours to obtain optically clear solution of PAN in DMF. InP material synthesized by the co-precipitation and hydrothermal method was added to DMF and sonicated for 18 hours at 50 °C subsequently to overcome their aggregation.

For the preparation of the composite solution, sonicated InP solution was added to the PAN solution in 75:25 wt.% respectively. Both the InP/PAN nanoparticles and InP/PAN nanospheres composite solutions were sonicated for 12 hours for thorough and homogeneous dispersion of InP nanomaterial in the polymer matrix.

2.3 Fabrication of InP nanofibers

Finally, the InP/PAN composite fibers were spun by the electrospinning of sonicated composite samples. The solution was filled in a syringe having metallic needle which was connected to a high DC voltage supply, and the copper collector was set at ground state potential. The distance between the needle tip and collector was 15 cm while a voltage of 25 kV was applied between them. The syringe was mounted on the pump and the flow rate of 0.1 ml/hr was maintained. The fibers thus produced were collected on FTO coated glass substrate and preserved in a desiccator because PAN is moisture sensitive. Ozone etching was carried out to obtain InP nanofibers.

2.4 Characterization Techniques

The surface morphology of the InP nanospheres were investigated by using SEM. SEM is very useful technique to study the surface morphology or topography of the material. Crystallinity of synthesized InP nanospheres sample was investigated by using XRD method. A very fine powder sample of InP nanospheres was subjected. Optical properties of InP nanospheres were investigated by SSPL, TRPL and Ultraviolet-Visible spectroscopy. In AFM, as the cantilever having a probe tip and a LASER source shining on probe tip. The tapping mode was used due to its capability of non-destructive high-resolution imaging of soft and fragile samples in ambient conditions. A minimal tip-sample force and an appropriate scan rate was adjusted for precise topographic imaging. The tip scanned over the sample and the deflection of the cantilever was quantified through the laser beam which was reflected off the backside of the cantilever and received by the photoelectric detector. These values were plotted as an amplitude map of the sample surface. Amplitude images tend to show edges of surface features well. The valuable information about important properties of nanofibers, such as hardness, elastic modulus and the adhesion between nanofibers and substrate were investigated.

3. Results and discussion

3.1 InP nanospheres

SEM images showing that InP nanospheres are moderately polydisperse in size with diameters ranging from 120-240 nm. The InP nanocrystallites had a tendency to aggregate [29]. It may be seen in Fig. 3 that nanospheres are in aggregated form. After the ultrasonic irradiation of

solution InP nanospheres in DMF, SEM image of sonicated InP nanospheres confirms the partial dispersion and breakage of the structures of a few nanospheres. SEM samples were prepared by drop casting and segregation.

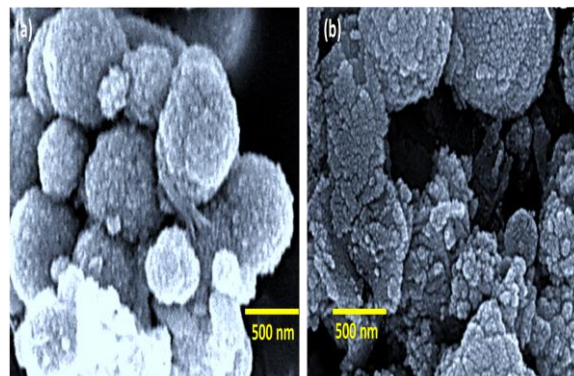


Fig. 3: SEM images of InP nanospheres, (a) before sonication and (b) after sonication

The Fig. 4 presents the X-ray diffractogram of the InP nanospheres. The diffraction pattern is in good agreement with that of crystalline zinc blende structure of InP, exhibiting the major peaks corresponding to the 111, 200, 220 and 311 reflection planes. The vertical red lines indicate the characteristic peak positions of bulk zinc blende structure of InP. The average crystallite size was estimated to be 153 nm.

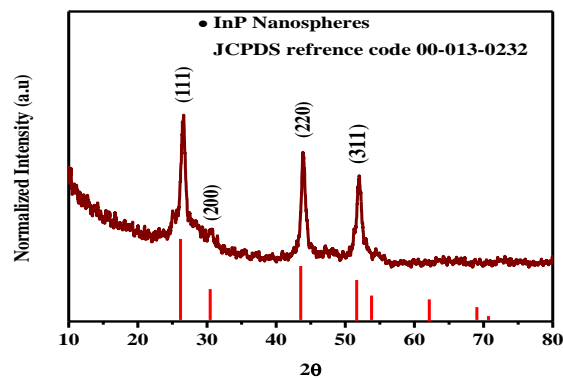


Fig. 4: X-ray diffractogram of InP nanospheres

For the TRPL spectroscopic investigation, a very dilute InP nanospheres solution in absolute methanol was prepared and the sample was excited with a laser pulse of 305 nm. Emission from various decay channels observed immediately after the laser excitation pulse, and only one wavelength (PL emission wavelength 634 nm) region was analyzed. Nanospheres comparatively larger in size, the electron wave function spread over a larger volume so the recombination probability is smaller and hence resulting in slower lifetime decay [30]. The experimental data from decay profile was fitted with a tri-exponential equation and the lifetime components are shown in Fig. 5.

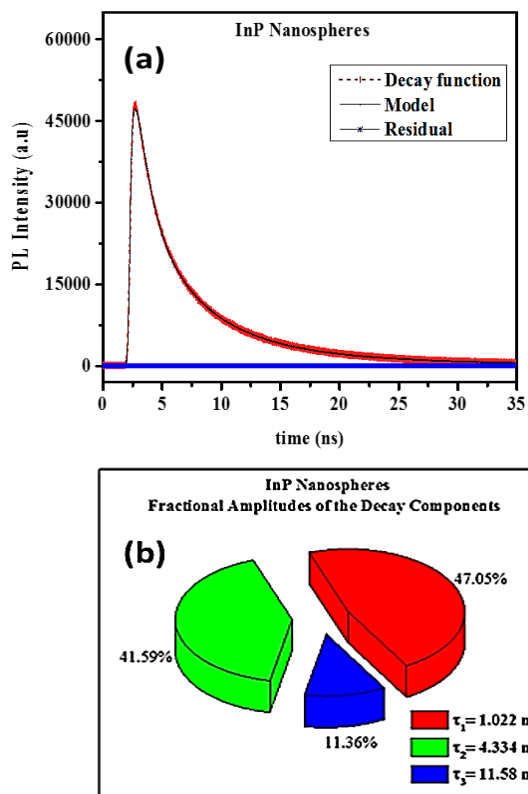


Fig. 5: (a) TRPL decay curve for InP Nanospheres and (b) Life time components InP nanospheres

Dilute solution of the synthesized InP nanospheres sample in absolute methanol was prepared for PL measurement and the sample was excited at 500 nm at room temperature as shown in Fig. 6. The PL emission spectrum of InP nanospheres were slightly shifted to longer wavelength 634 nm (1.96 eV) than the absorption band edge 626 nm (1.98 eV), it may be due to polydispersity in size of InP nanospheres [31].

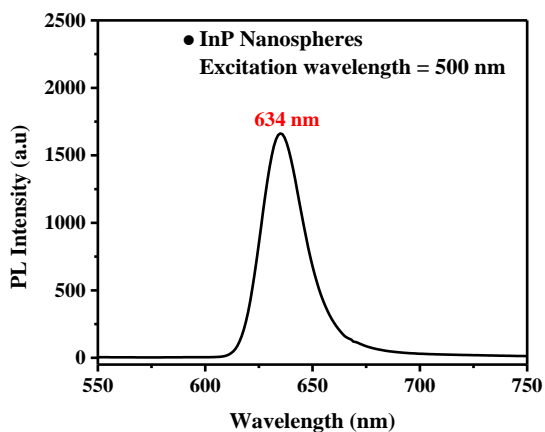


Fig. 6: PL emission spectrum of InP nanospheres

Dilute solution of the synthesized InP nanospheres sample was prepared in methanol by

ultrasonic irradiation for UV-Vis absorption measurement. The first excitonic absorption wavelength was observed at 626 nm for InP nanospheres. The band edge position with clear excitonic shoulder in optical absorption profile is suggestive of growth with a narrow size distribution. From absorption spectrum of the synthesized InP Nanospheres they were observed to exhibit the blue shift of about 292 nm as compared to the bulk InP (918 nm) absorption value as shown in Fig. 7. The estimated band gap of synthesized InP nanospheres was ~ 1.98 eV (as shown in Fig. 7) which is larger than the band gap of bulk InP (1.34 eV) [32].

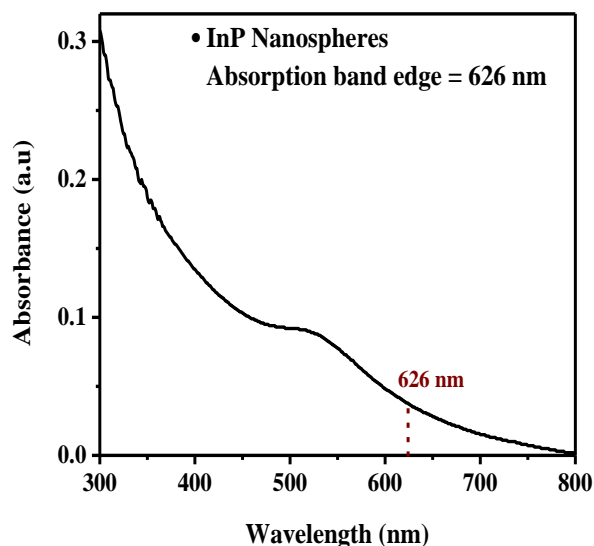


Fig 7: (a) UV/Vis absorption spectrum of InP nanospheres

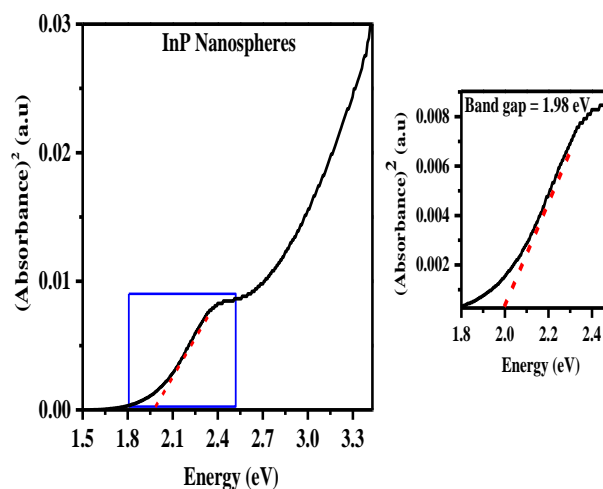


Fig. 7: (b) Optical band gap calculation of InP nanospheres

3.2 InP/PAN composite nanofibers

Surface studies on InP/PAN composite nanofibers were studied by SEM and AFM. In Fig. 8, InP/PAN composite nanofibers with clear polymer coating were successfully fabricated by electrospinning method.

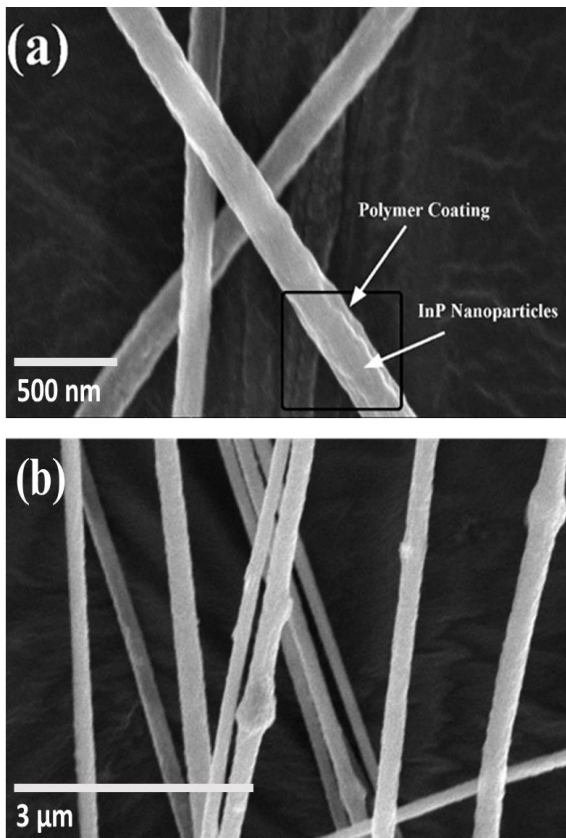


Fig. 8: InP/PAN nanospheres composite nanofibers (a) at high resolution (b) at low resolution

3.3 InP nanofibers

Fabricated InP/PAN nanofibers were collected on FTO (fluorine doped tin oxide) coated glass substrate. The polymer coated InP nanofibers were then placed into an ozone chamber and ozone etching was carried out to expose the surface of InP as it can be seen in Fig. 9 the polymer coating was almost decomposed and nanoparticles were aligned uniformly in the form of fibers. Thermal degradation of polymer was avoided as it results in carbonization and the carbon contents in nanofibers passively inactivate their optical properties. The FTO supported InP nanofibers were then calcined at 400 °C and the fibers stiffness was analyzed by atomic force microscopy.

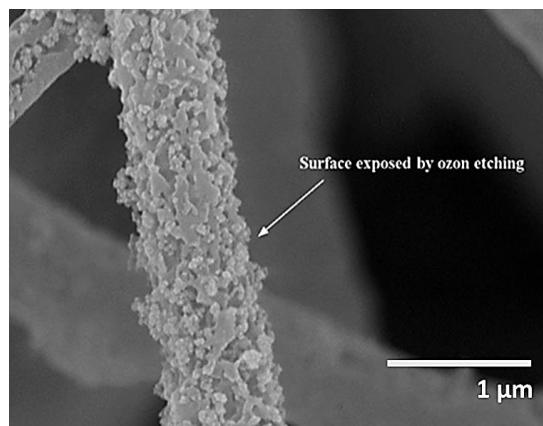


Fig. 9: InP nanospheres based nanofibers after ozone etching

Phase imaging involves monitoring the change in phase offset, or phase angle, of the input signal with respect to the phase offset of the oscillating cantilever. The changes in phase offset was due to different amounts of damping experienced by the probe tip. These differences were plotted as phase image. The Fig. 11 showing phase image of nanospheres based nanofibers supported on FTO coated glass substrate.

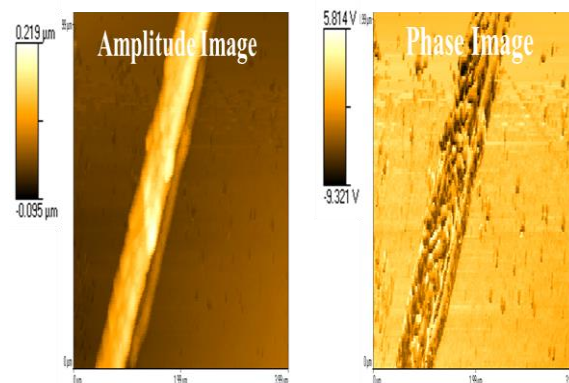


Fig. 10: AFM amplitude and phase images of InP nanosphere based nanofibers

4. Conclusions

InP nanostructures were fabricated by solvothermal (nanosphere) and electrospinning (nanofibers) methods. The synthesis of InP nanospheres by solvothermal methods resulted in well crystalline InP nanostructures. The reflection planes in diffractograms of all the synthesized InP nanostructures were in good agreement with cubic zinc blende crystal structure of InP. InP nanofibers were fabricated by electrospinning method and FTO supported nanofibers when analyzed by AFM, it revealed that InP nanosphere based nanofibers were uniformly aligned. Ultrasonic irradiation effect was studied for InP nanospheres. By SEM analysis the aggregates of InP

nanospheres showed their partial dispersion and breakage of few nanospheres. A linear relationship in optical properties were observed, as the long tail effect in photoluminescence spectra were due to the (presence of shallow and deep traps within the band gap) surface defects and time resolved kinetic profile supports the SSPL results. It was observed that PL decay profile for different nanostructured materials provide some insight as the size of nanostructures affects the exciton lifetime, with large sized nanostructures the electron wave function spread over a larger volume and the recombination probability is smaller, resulting in shorter PL lifetimes.

5. References

- [1] Kim, T., Lee, D., & Yoon, Y. (2000). Microstructural, electrical, and optical properties of SnO₂ nanocrystalline thin films grown on InP (100) substrates for applications as gas sensor devices. *Journal of applied Physics*, 88(6), 3759-3761.
- [2] Ribordy, G., Gautier, J.-D., Zbinden, H., & Gisin, N. (1998). Performance of InGaAs/InP avalanche photodiodes as gated-mode photon counters. *Applied Optics*, 37(12), 2272-2277.
- [3] Soda, H., Kotaki, Y., Sudo, H., Ishikawa, H., Yamakoshi, S., & Imai, H. (1987). Stability in single longitudinal mode operation in GaInAsP/InP phase-adjusted DFB lasers. *IEEE Journal of Quantum Electronics*, 23(6), 804-814.
- [4] Fiorentino, M., Voss, P. L., Sharping, J. E., & Kumar, P. (2002). All-fiber photon-pair source for quantum communications. *IEEE Photonics Technology Letters*, 14(7), 983-985.
- [5] Baba, T., Fukaya, N., & Yonekura, J. (1999). Observation of light propagation in photonic crystal optical waveguides with bends. *Electronics letters*, 35(8), 654-655.
- [6] Hattendorf, M., Hartmann, Q., Richards, K., & Feng, M. (2002). Sub-micron scaling of high-speed InP/InGaAs SHBTs grown by MOCVD using carbon as the p-Type dopant. Paper presented at the 2002 GaAs MANTECH Conf. Dig. Ppr.
- [7] Wallentin, J., Anttu, N., Asoli, D., Huffman, M., Åberg, I., Magnusson, M. H., Witzigmann, B. (2013). InP nanowire array solar cells achieving 13.8% efficiency by exceeding the ray optics limit. *Science*, 339(6123), 1057-1060.
- [8] Abrahams, M., Braunstein, R., & Rosi, F. (1959). Thermal, electrical and optical properties of (In, Ga) as alloys. *Journal of Physics and Chemistry of Solids*, 10(2-3), 204-210.
- [9] Bar-Joseph, I., Klingshirn, C., Miller, D., Chemla, D., Koren, U., & Miller, B. (1987). Quantum-confined Stark effect in InGaAs/InP quantum wells grown by organometallic vapor phase epitaxy. *Applied physics letters*, 50(15), 1010-1012.
- [10] Baskoutas, S., & Terzis, A. F. (2006). Size-dependent band gap of colloidal quantum dots. *Journal of applied Physics*, 99(1), 013708.
- [11] Dresselhaus, M., & Thomas, I. (2001). Alternative energy technologies. *Nature*, 414(6861), 332-337.
- [12] Leijtens, X. (2011). JePPIX: the platform for Indium Phosphide-based photonics. *IET optoelectronics*, 5(5), 202-206.
- [13]. Hangarter, C. M., & Myung, N. V. (2005). Magnetic alignment of nanowires. *Chemistry of materials*, 17(6), 1320-1324.
- [14] Duan, X., Huang, Y., Cui, Y., Wang, J., & Lieber, C. M. (2001). Indium phosphide nanowires as building blocks for nanoscale electronic and optoelectronic devices. *Nature*, 409(6816), 66-69.
- [15] Thakur, M. (1977). Gallium-67 and indium-111 radiopharmaceuticals. *The International journal of applied radiation and isotopes*, 28(1-2), 183-201.
- [16] Ghaderi, S., Ramesh, B., & Seifalian, A. M. (2011). Fluorescence nanoparticles “quantum dots” as drug delivery system and their toxicity: a review. *Journal of drug targeting*, 19(7), 475-486.
- [17] Siddiqui, I. R., Singh, A., Shamim, S., Srivastava, V., Singh, P. K., Yadav, S., & Singh, R. K. (2010). Recyclable Indium (III) Chloride Catalyzed Site-Selective Double Substitution in One Pot for the Synthesis of Isatin N-Ribonucleosides under Microwave Irradiation. *Synthesis*, 2010(10), 1613-1616.
- [18] Rodrigo, S. M., Cunha, A., Pozza, D. H., Blaya, D. S., Moraes, J. F., Weber, J. B. B., & de Oliveira, M. G. (2009). Analysis of the systemic effect of red and infrared laser

- therapy on wound repair. *Photomedicine and laser surgery*, 27(6), 929-935.
- [19] Andriano, K., Tabata, Y., Ikada, Y., & Heller, J. (1999). In vitro and in vivo comparison of bulk and surface hydrolysis in absorbable polymer scaffolds for tissue engineering. *Journal of biomedical materials research*, 48(5), 602-612.
- [20] Olmedo, D. G., Tasat, D. R., Duffó, G., Guglielmotti, M. B., & Cabrini, R. L. (2009). The issue of corrosion in dental implants: a review. *Acta Odontol Latinoam*, 22(1), 3-9.
- [21] Huang, Z.-M., Zhang, Y.-Z., Kotaki, M., & Ramakrishna, S. (2003). A review on polymer nanofibers by electrospinning and their applications in nanocomposites. *Composites science and technology*, 63(15), 2223-2253.
- [22] Nair, L. S., Bhattacharyya, S., Bender, J. D., Greish, Y. E., Brown, P. W., Allcock, H. R., & Laurencin, C. T. (2004). Fabrication and optimization of methylphenoxy substituted polyphosphazene nanofibers for biomedical applications. *Biomacromolecules*, 5(6), 2212-2220.
- [23] Ryu, Y. J., Kim, H. Y., Lee, K. H., Park, H. C., & Lee, D. R. (2003). Transport properties of electrospun nylon 6 nonwoven mats. *European Polymer Journal*, 39(9), 1883-1889.
- [24] Fong, H., Chun, I., & Reneker, D. (1999). Beaded nanofibers formed during electrospinning. *Polymer*, 40(16), 4585-4592.
- [25] Tan, S., Inai, R., Kotaki, M., & Ramakrishna, S. (2005). Systematic parameter study for ultra-fine fiber fabrication via electrospinning process. *Polymer*, 46(16), 6128-6134.
- [26] Son, W. K., Youk, J. H., Lee, T. S., & Park, W. H. (2004). The effects of solution properties and polyelectrolyte on electrospinning of ultrafine poly (ethylene oxide) fibers. *Polymer*, 45(9), 2959-2966.
- [27] Deitzel, J. M., Kleinmeyer, J., Harris, D., & Tan, N. B. (2001). The effect of processing variables on the morphology of electrospun nanofibers and textiles. *Polymer*, 42(1), 261-272.
- [28] Hansma, H. G., & Hoh, J. H. (1994). Biomolecular imaging with the atomic force microscope. *Annual review of biophysics and biomolecular structure*, 23(1), 115-140.
- [29] Pileni, M.-P. (2003). The role of soft colloidal templates in controlling the size and shape of inorganic nanocrystals. *Nature materials*, 2(3), 145.
- [30] Zavelani-Rossi, M., Lupo, M. G., Tassone, F., Manna, L., & Lanzani, G. (2010). Suppression of biexciton Auger recombination in CdSe/CdS dot/rods: role of the electronic structure in the carrier dynamics. *Nano Letters*, 10(8), 3142-3150.
- [31] Crooker, S., Hollingsworth, J., Tretiak, S., & Klimov, V. (2002). Spectrally resolved dynamics of energy transfer in quantum-dot assemblies: Towards engineered energy flows in artificial materials. *Physical review letters*, 89(18), 186802.
- [32] Micic, O., Sprague, J., Curtis, C., Jones, K., Machol, J., Nozik, A., Peyghambarian, N. (1995). Synthesis and characterization of InP, GaP, and GaInP₂ quantum dots. *The Journal of Physical Chemistry*, 99(19), 7754-7759.